J Physiol 590.23 (2012) pp 6093–6108

The Journal of Physiology

β-Adrenergic stimulation increases the intra-sarcoplasmic reticulum Ca^{2+} threshold for Ca^{2+} wave generation

Timothy L. Domeier, Joshua T. Maxwell and Lothar A. Blatter

Department of Molecular Biophysics and Physiology, Rush University Medical Center, Chicago, IL, USA

Key points

- In the heart, Ca^{2+} waves are arrhythmogenic spontaneous sarcoplasmic reticulum (SR) Ca^{2+} release events that arise when the Ca^{2+} content in the SR reaches a critical threshold level.
- β-Adrenergic signalling induces Ca^{2+} waves in cardiac myocytes, but it remains unclear if this is due to a decrease in the Ca^{2+} wave threshold or more simply due to an increase in SR Ca^{2+} content.
- We used direct, dynamic measurement of SR Ca^{2+} levels to show that the Ca^{2+} wave threshold is unexpectedly increased during β-adrenergic stimulation.
- Our data show that the primary cause of Ca^{2+} waves following acute β-adrenergic stimulation is the increase in SR Ca^{2+} content and not a decrease in the Ca^{2+} wave threshold.
- We propose that the elevation of the Ca^{2+} wave threshold represents a protective mechanism against arrhythmogenic events during periods of β-adrenergic stimulation.

Abstract β-Adrenergic signalling induces positive inotropic effects on the heart that associate with pro-arrhythmic spontaneous Ca^{2+} waves. A threshold level of sarcoplasmic reticulum (SR) Ca^{2+} ($[Ca^{2+}]_{SR}$) is necessary to trigger Ca^{2+} waves, and whether the increased incidence of Ca^{2+} waves during β-adrenergic stimulation is due to an alteration in this threshold remains controversial. Using the low-affinity Ca^{2+} indicator fluo-5N entrapped within the SR of rabbit ventricular myocytes, we addressed this controversy by directly monitoring $[Ca^{2+}]_{SR}$ and Ca^{2+} waves during β-adrenergic stimulation. Electrical pacing in elevated extracellular Ca^{2+} ($[Ca^{2+}]_o = 7$ mM) was used to increase $[Ca^{2+}]_{SR}$ to the threshold where Ca^{2+} waves were consistently observed. The β-adrenergic agonist isoproterenol (ISO; 1 μM) increased $[Ca^{2+}]_{SR}$ well above the control threshold and consistently triggered Ca^{2+} waves. However, when $[Ca^{2+}]_{SR}$ was subsequently lowered in the presence of ISO (by lowering $[Ca^{2+}]_o$ to 1 mM and partially inhibiting sarcoplasmic/endoplasmic reticulum calcium ATPase with cyclopiazonic acid or thapsigargin), Ca^{2+} waves ceased to occur at a $[Ca^{2+}]_{SR}$ that was higher than the control threshold. Furthermore, for a set $[Ca^{2+}]_{SR}$ level the refractoriness of wave occurrence (Ca^{2+} wave latency) was prolonged during β-adrenergic stimulation, and was highly dependent on the extent that $[Ca]_{SR}$ exceeded the wave threshold. These data show that acute β-adrenergic stimulation increases the $[Ca^{2+}]_{SR}$ threshold for Ca^{2+} waves, and therefore the primary cause of Ca^{2+} waves is the robust increase in $[Ca^{2+}]_{SR}$ above this higher threshold level. Elevation of the $[Ca^{2+}]_{SR}$ wave threshold and prolongation of wave latency represent potentially protective mechanisms against pro-arrhythmogenic Ca^{2+} release during β-adrenergic stimulation.

(Received 4 May 2012; accepted after revision 10 September 2012; first published online 17 September 2012)
Corresponding author L. A. Blatter: Department of Molecular Biophysics and Physiology, Rush University Medical Center, 1750 W. Harrison Street, Chicago, IL 60612, USA. Email: lothar_blatter@rush.edu

DOI: 10.1113/jphysiol.2012.236117

Abbreviations AP, action potential; $[Ca^{2+}]_i$, cytosolic free calcium concentration; $[Ca^{2+}]_o$, extracellular free calcium concentration; $[Ca^{2+}]_{SR}$, intra-sarcoplasmic reticulum free calcium concentration; CICR, calcium-induced calcium release; CPA, cyclopiazonic acid; CPVT, catecholaminergic polymorphic ventricular tachycardia; CRU, calcium release unit; DMSO, dimethyl sulfoxide; ISO, isoproterenol; LTCC, L-type calcium channel; RyR, ryanodine receptor; SERCA, sarcoplasmic/endoplasmic reticulum calcium ATPase; SR, sarcoplasmic reticulum; TG, thapsigargin.

Introduction

Cardiac contraction is triggered via Ca^{2+}-induced Ca^{2+} release (CICR), where influx of Ca^{2+} into the cardiomyocyte through L-type Ca^{2+} channels (LTCCs) opens ryanodine receptor (RyR) Ca^{2+} release channels in the junctional sarcoplasmic reticulum (SR) membrane and initiates coordinated release of Ca^{2+} from the SR Ca^{2+} store. SR Ca^{2+} release can also occur spontaneously during diastole. Diastolic Ca^{2+} release is detrimental to cardiac performance as it impairs relaxation, reduces the concentration of Ca^{2+} within the SR ($[Ca^{2+}]_{SR}$) and predisposes the heart to arrhythmia. One highly arrhythmogenic form of diastolic Ca^{2+} release is the Ca^{2+} wave, where Ca^{2+} that is spontaneously released from an SR Ca^{2+} release unit (CRU, formed by a cluster of RyRs) diffuses to neighbouring CRUs and triggers regenerative and propagating CICR independently of the cardiac action potential (AP) (Stern *et al.* 1988). Extrusion of Ca^{2+} that is released during a Ca^{2+} wave via the electrogenic Na^+–Ca^{2+} exchange mechanism (Kass *et al.* 1978; Fedida *et al.* 1987) has a strong depolarizing effect on the diastolic membrane potential and underlies arrhythmogenic delayed afterdepolarizations (Capogrossi *et al.* 1987; Schlotthauer & Bers, 2000; Fujiwara *et al.* 2008). It is therefore of paramount importance to understand the mechanisms for Ca^{2+} wave generation in the heart.

A considerable amount of evidence has emerged that a distinct 'overload' $[Ca^{2+}]_{SR}$ is necessary to trigger Ca^{2+} waves, and this level has been termed the Ca^{2+} wave threshold (Díaz *et al.* 1997*b*; Venetucci *et al.* 2007) or store overload-induced Ca^{2+} release threshold (Jiang *et al.* 2004). The Ca^{2+} wave threshold is altered by agents that modulate RyR activity, with channel activators (e.g. caffeine) and inhibitors (e.g. tetracaine) decreasing (Venetucci *et al.* 2007; Kong *et al.* 2008) and increasing (Overend *et al.* 1997) the threshold, respectively. In animal models of heart failure where RyR channel activity is increased, the Ca^{2+} wave threshold is decreased (Belevych *et al.* 2012; Maxwell *et al.* 2012) and this may play a role in the arrhythmogenesis associated with these models. Furthermore, investigations of RyR mutations associated with catecholaminergic polymorphic ventricular tachycardia (CPVT) have shown that gain-of-function mutations (reviewed by Priori & Chen, 2011) result in a decrease in the Ca^{2+} wave threshold and increased incidence of arrhythmogenic Ca^{2+} release following increases in $[Ca^{2+}]_{SR}$ [e.g. in response to cardiac glycosides (Sedej *et al.* 2010) or β-adrenergic stimulation (Kashimura *et al.* 2010)]. Interestingly, although the Ca^{2+} wave threshold is lower in cardiomyocytes from CPVT RyR R4496C mutant mice than in wild-type controls, β-adrenergic stimulation *increases* the Ca^{2+} wave threshold in R4496C myocytes (Kashimura *et al.* 2010). Thus, the likely factor triggering Ca^{2+} waves in response to catecholamines in this CPVT model is the sudden increase in $[Ca^{2+}]_{SR}$ and not an acute lowering of the Ca^{2+} wave threshold. A similar increase in the Ca^{2+} wave threshold in response to β-adrenergic signalling was observed in wild-type mouse cardiomyocytes (Kashimura *et al.* 2010; Stokke *et al.* 2010*a*), suggesting that this effect is not unique to disease models. Contrasting with these data are investigations that show that β-adrenergic stimulation increases diastolic SR Ca^{2+} release in the form of Ca^{2+} sparks (Zhou *et al.* 2009; Ogrodnik & Niggli, 2010), SR Ca^{2+} leak (Curran *et al.* 2007; Bovo *et al.* 2012; Ullrich *et al.* 2012) and Ca^{2+} waves (Curran *et al.* 2010) at a similar or lower level of SR Ca^{2+} content (which intuitively should translate into a *decrease* in the Ca^{2+} wave threshold). Additionally, selective activation of signalling molecules acting downstream of β-adrenergic stimulation (Guo *et al.* 2006; Terentyev *et al.* 2008) or phosphomimetic mutation of target phosphorylation sites on the RyR (Shan *et al.* 2010; van Oort *et al.* 2010) have all been shown to augment SR Ca^{2+} release and predispose the heart to arrhythmia. Thus, it remains unclear and highly controversial whether Ca^{2+} waves during β-adrenergic stimulation are due to direct alterations in the Ca^{2+} wave threshold or more simply due to the increase in $[Ca^{2+}]_{SR}$ that occurs concomitant with activation of the signalling pathway.

Measurement of the Ca^{2+} wave threshold in cardiomyocytes during β-adrenergic stimulation is experimentally challenging due to the enhanced activity of multiple Ca^{2+} handling proteins, which hinders targeted and controlled examination of the Ca^{2+} wave threshold. To gain new insight into the mechanisms underlying Ca^{2+} waves during β-adrenergic stimulation we utilized direct, dynamic fluorescent measurement of $[Ca^{2+}]_{SR}$ and the Ca^{2+} wave threshold in acutely isolated rabbit ventricular myocytes. We found that β-adrenergic stimulation *increases* the Ca^{2+} wave threshold, which may serve to protect the heart from arrhythmogenic Ca^{2+} release as $[Ca^{2+}]_{SR}$ increases during sympathetic nervous system activation.

Part of this work has been presented previously in abstract form (Domeier & Blatter, 2010; Domeier *et al.* 2011).

Methods

Solutions and chemicals

All reagents were purchased from Sigma-Aldrich (St. Louis, MO, USA) unless otherwise noted. Normal Tyrode solution contained (in mM): 135 NaCl, 4 KCl, 2 $CaCl_2$, 1 $MgCl_2$, 10 D-glucose and 10 Hepes (pH 7.4 with NaOH). Tyrode solutions with altered extracellular free calcium concentration ($[Ca^{2+}]_o$) were prepared using iso-osmotic substitution of $CaCl_2$ and NaCl. Isoproterenol (ISO) was prepared daily as a stock solution of 100 mM (in H_2O, maintained at 4°C), diluted in Tyrode solution immediately prior to experimental procedures and used within 30 min. Cyclopiazonic acid (CPA) and thapsigargin (TG) were dissolved in DMSO and diluted to working concentrations in Tyrode solution. All experiments were performed with appropriate vehicle controls. All experiments were conducted at room temperature (22–24°C).

Cardiac myocyte isolation

Left ventricular myocytes were isolated from male New Zealand White rabbits (30 animals, 2.5 kg, Myrtle's Rabbitry, Thompsons Station, TN, USA). Rabbits were anaesthetized with sodium pentobarbital (50 mg kg^{-1}) and hearts were rapidly excised and retrogradely perfused with a nominally Ca^{2+}-free Tyrode solution for 10 min, followed by a minimal essential Eagle's medium (MEM) solution with 20 μM Ca^{2+} and 45 μg ml^{-1} Liberase Blendzyme TH (Roche Applied Science, Indianapolis, IN, USA) for 20 min all at 37°C. The left ventricular free wall tissue was minced, filtered and washed in MEM solution containing 50 μM Ca^{2+} and 10 mg ml^{-1} BSA. Isolated myocytes were maintained in MEM solution with 50 μM Ca^{2+} at room temperature until Ca^{2+} indicator dye loading procedures. All protocols were approved by the Institutional Animal Care and Use Committee at Rush University, and comply with US and UK regulations on animal experimentation (Drummond, 2009).

Intra-SR Ca^{2+} measurements

Ventricular myocytes were incubated with 10 μM of membrane-permeant fluo-5N/AM (Molecular Probes-Life Technologies, Grand Island, NY, USA) for 2.5 h at 37°C to promote accumulation of dye within the SR (see Fig. 2*A*). Following a 30 min wash at 37°C, myocytes were equilibrated to room temperature and plated on laminin-coated coverslips for imaging experiments. Laser scanning fluorescence confocal microscopy was performed using the resonant scan head of a Nikon A1R system (Nikon Instruments Inc., Melville, NY, USA) in frame scan mode (60 frames s^{-1} at 256 × 512 pixels, 400 nm per pixel). Fluo-5N was excited using the 488 nm line of the argon ion laser and emission was recorded at 500–530 nm. Low laser excitation intensities and limited recording times were used to minimize photobleaching of the fluo-5N indicator. Although generally negligible, in some experiments with extended recording times (e.g. Fig. 3*A*) photobleaching did occur and these recordings were corrected using control bleach rates (single exponential fits) obtained from each cell under steady-state conditions. Changes in $[Ca^{2+}]_{SR}$ are presented as $(F-F_{Min})/(F_{Max}-F_{Min})$ or calibrated as $[Ca^{2+}]_{SR} = [400\ \mu M \times (F-F_{Min})/(F_{Max}-F)]$ (Shannon *et al.* 2003; Zima *et al.* 2011). F_{Min} is the quench-corrected (15%) fluorescence value following complete emptying of the SR with 10 mM caffeine, and F_{Max} is taken as the diastolic fluorescence at 1 Hz pacing in the presence of 1 μM ISO.

Cytosolic Ca^{2+} ($[Ca^{2+}]_i$) measurements, indo-1

For ratiometric epifluorescence $[Ca^{2+}]_i$ measurements, myocytes were loaded with 5 μM indo-1/AM (Molecular Probes-Life Technologies) for 10 min followed by a 30 min wash, all at room temperature. Single myocytes were exposed to 360 nm light to excite indo-1, and fluorescence emission was simultaneously monitored at 410 nm (F_{410}) and 485 nm (F_{485}). Fluorescence emission at each wavelength was background subtracted and $[Ca^{2+}]_i$ is presented as the indo-1 ratio ($R = F_{410}/F_{485}$) or change in indo-1 ratio ($\Delta R = R_{peak} - R_{baseline}$).

Cytosolic Ca^{2+} measurements, rhod-2

Myocytes preloaded with fluo-5N were subsequently loaded with the spectrally distinct Ca^{2+} indicator rhod-2/AM (Molecular Probes-Life Technologies, 5 μM, 10 min loading time, 10 min wash, all at room temperature) to monitor cytosolic Ca^{2+} waves simultaneously with $[Ca^{2+}]_{SR}$. Laser scanning fluorescence confocal microscopy was performed (Nikon A1R, 60 frames s^{-1}) with rhod-2 excitation at 543 nm and fluorescence emission recorded at >600 nm. Rhod-2 fluorescence signals are presented as F/F_0, where F_0 is the diastolic fluorescence at the start of each experimental recording.

Experimental protocols to determine the Ca^{2+} wave threshold

Control conditions. Two series of experiments were conducted to determine the Ca^{2+} wave threshold. In one series, the Ca^{2+} wave threshold was determined based on

direct measurement of $[Ca^{2+}]_{SR}$ using fluo-5N, whereas the second series relied on cytosolic $[Ca^{2+}]_i$ measurements (with indo-1) in response to caffeine challenge to estimate SR Ca^{2+} content. Because rabbit ventricular myocytes did not typically exhibit Ca^{2+} waves under control conditions ($[Ca^{2+}]_o = 2$ mM), a high extracellular Ca^{2+} solution was applied ($[Ca^{2+}]_o = 7$ mM). In both series of experiments rabbit ventricular myocytes underwent several consecutive experimental trials defined here as an episode consisting of electrical field stimulation of cells for a period of 30–60 s, followed by 8 s of rest. The stimulation–rest protocol was repeated at incrementally increasing pacing frequencies (0.05–0.2 Hz increments) to increase $[Ca^{2+}]_{SR}$ (see Fig. 3*B*) until Ca^{2+} waves were observed during the rest period. In fluo-5N experiments the $[Ca^{2+}]_{SR}$ where waves were observed was defined as the '*wave* threshold' and the $[Ca^{2+}]_{SR}$ at the preceding lower frequency where waves were not observed was defined as the '*no-wave* threshold'. Control measurements confirmed that the control *wave* and *no-wave* thresholds were stable and reproducible over time. Additionally, in experiments where waves were observed, SR Ca^{2+} refilling time and wave latency were calculated. SR Ca^{2+} refilling time was defined as the interval between the AP-induced depletion nadir (minimum $[Ca^{2+}]_{SR}$ value) and the time point when $[Ca^{2+}]_{SR}$ recovered to the $[Ca^{2+}]_{SR}$ observed prior to the depletion (dark grey in Fig. 6*A*). Wave latency was calculated as the interval between the time point when $[Ca^{2+}]_{SR}$ recovered from an AP-induced depletion and the onset of the wave (light grey in Fig. 6*A*). In indo-1 experiments the SR Ca^{2+} content associated with a particular stimulation frequency was determined in a separate pacing train using the amplitude of the Ca^{2+} transient in response to 10 mM caffeine. This value was determined immediately following cessation of pacing.

β-Adrenergic stimulation. In all experiments β-adrenergic stimulation (ISO, 5 min) increased $[Ca^{2+}]_{SR}$ compared with control conditions and triggered Ca^{2+} waves. To determine the critical $[Ca^{2+}]_{SR}$ threshold level where Ca^{2+} waves occurred (or ceased to occur when $[Ca^{2+}]_{SR}$ was lowered) a protocol was applied that resulted in a gradual decrease of $[Ca^{2+}]_{SR}$ levels after the initial increase, all in the maintained presence of ISO. For this, $[Ca^{2+}]_o$ was lowered (as indicated) and sarcoplasmic/endoplasmic reticulum calcium ATPase (SERCA) was partially blocked by CPA or TG while β-adrenergic stimulation was maintained. In the fluo-5N experiments this protocol allowed for direct assessment of the $[Ca^{2+}]_{SR}$ where waves occurred during β-adrenergic stimulation, with subsequent paired comparison with the respective control threshold levels. With the indo-1 experimental approach *wave* and *no-wave* thresholds under control conditions were determined as described above. However, in the presence of ISO+CPA only *no-wave* data points were used for analysis. This analysis design was implemented because the indirect assessment of SR Ca^{2+} content from the caffeine-induced cytosolic Ca^{2+} transient would have to occur *after* a Ca^{2+} wave. With CPA or TG present the amount of $[Ca^{2+}]_{SR}$ remaining in the SR following a Ca^{2+} wave is significantly lower than that which preceded the wave due to the impaired reuptake by SERCA (Díaz *et al.* 1997*a*; Domeier *et al.* 2010; see Figs 2*B*, 3*A* and 4*A*), i.e. application of caffeine after a Ca^{2+} wave would grossly underestimate the wave threshold.

Statistics and data analysis

Only rod-shaped myocytes with clear striations were used for experimental protocols. Approximately 20% of myocytes exhibited visible damage during the repetitive stimulation/rest protocols (e.g. membrane blebbing or irreversible cellular contracture). These myocytes were not utilized for data analysis. Data are presented as individual observations from single myocytes or as mean ± standard error of the mean (SEM). Statistical comparisons were performed using Student's *t* test for paired or unpaired data, with significance set at $P < 0.05$. The number of individual cells or experimental trials is given as *n* as indicated.

Results

In this investigation we tested the hypothesis that β-adrenergic receptor stimulation alters the intra-SR Ca^{2+} threshold for spontaneous Ca^{2+} waves. For this, we monitored spontaneous Ca^{2+} waves that occurred during rest from steady-state electrical stimulation. A major difficulty associated with studies of SR Ca^{2+} release following activation of β-adrenergic stimulation is that intracellular Ca^{2+} handling is profoundly altered by this signalling pathway, most notably an increase in Ca^{2+} entry into the cell via the LTCC (Tsien *et al.* 1986) and an increase in SR Ca^{2+} content via effects on phospholamban and the SERCA pump (Kranias & Solaro, 1982; Lindemann *et al.* 1983). Because of these effects, it becomes experimentally difficult to control both $[Ca^{2+}]_i$ and $[Ca^{2+}]_{SR}$, which is essential when monitoring SR Ca^{2+} release as RyR gating is influenced by both cytosolic and intra-luminal $[Ca^{2+}]$ (Fill & Copello, 2002). We therefore defined experimental conditions where Ca^{2+} cycling (in particular $[Ca^{2+}]_i$) was the same between control conditions and in the presence of β-adrenergic stimulation (1 μM ISO, 5 min), and reasoned that if during rest from electrical stimulation steady-state $[Ca^{2+}]_i$ is equivalent between the two respective conditions then the $[Ca^{2+}]_{SR}$ where Ca^{2+} waves occur will directly reflect the intra-SR Ca^{2+} wave threshold.

Acute application of ISO led to an increase in Ca^{2+} transient amplitude (Fig. 1*A* and *C*, arrows indicate electrically evoked Ca^{2+} transients), resting $[Ca^{2+}]_i$ (Fig. 1*A* and *D*) and SR Ca^{2+} content as assessed from the amplitude of the $[Ca^{2+}]_i$ increase in response to 10 mM caffeine (Fig. 1*B* and *E*). Under these conditions, spontaneous Ca^{2+} waves were frequently observed during the rest period following steady-state stimulation (Fig. 1*A*, star). Subsequent addition of a low extracellular Ca^{2+} solution ($[Ca^{2+}]_o = 100\ \mu M$) containing ISO and the SERCA inhibitor CPA (7.5 μM) returned critical parameters of cellular Ca^{2+} handling to levels observed under control conditions, with Ca^{2+} transient amplitude (Fig. 1*C*), resting $[Ca^{2+}]_i$ (Fig. 1*D*) and SR Ca^{2+} content (Fig. 1*E*) becoming similar to the original control conditions.

We next loaded the SR of cardiomyocytes with the low affinity Ca^{2+} indicator fluo-5N to directly and dynamically monitor the $[Ca^{2+}]_{SR}$ when waves occur. Figure 2*A* shows the typical fluo-5N SR staining pattern. Based on observations of increased SR Ca^{2+} release in the form of Ca^{2+} sparks (Zhou *et al.* 2009; Ogrodnik & Niggli, 2010), Ca^{2+} leak (Curran *et al.* 2010; Bovo *et al.* 2012; Ullrich *et al.* 2012) and Ca^{2+} waves (Curran *et al.* 2007) in the presence of β-adrenergic stimulation, our initial hypothesis was that ISO would *decrease* the $[Ca^{2+}]_{SR}$ threshold where waves occurred (i.e. Ca^{2+} waves would be observed in the presence of ISO at a $[Ca^{2+}]_{SR}$ at or below the level where waves were *not* observed under control conditions). In rabbit ventricular myocytes Ca^{2+} waves were not typically observed under control conditions with 2 mM $[Ca^{2+}]_o$ (Fig. 2*Ba* and *D*). However Ca^{2+} waves could be triggered using a low concentration (250 μM) of caffeine (Fig. 2*Bb* and *D*), a RyR agonist that sensitizes the release channel to Ca^{2+} and lowers the intra-SR Ca^{2+} threshold for Ca^{2+} waves (Venetucci *et al.* 2007; Kong *et al.* 2008). Application of ISO caused a large increase in $[Ca^{2+}]_{SR}$ (Fig. 2*Bc* and *C*) and Ca^{2+} waves were observed (Fig. 2*Bc* and D). We then applied ISO+CPA ($[Ca^{2+}]_o = 100\ \mu M$) to lower $[Ca^{2+}]_{SR}$. When $[Ca^{2+}]_{SR}$ decreased to a similar level as under control conditions no Ca^{2+} waves were observed (Fig. 2*Bd* and *D*). Subsequent addition of 250 μM caffeine to myocytes treated with ISO+CPA triggered Ca^{2+} waves similarly to control conditions (Fig. 2*Be* and *D*). In summary, the data shown in Figs 1 and 2 indicate that under conditions of identical $[Ca^{2+}]_i$ and $[Ca^{2+}]_{SR}$ ISO stimulation failed to increase the propensity of Ca^{2+} waves and therefore does not appear to lower the Ca^{2+} wave threshold.

We next tested the alternative hypothesis that β-adrenergic stimulation *increases* the $[Ca^{2+}]_{SR}$ threshold

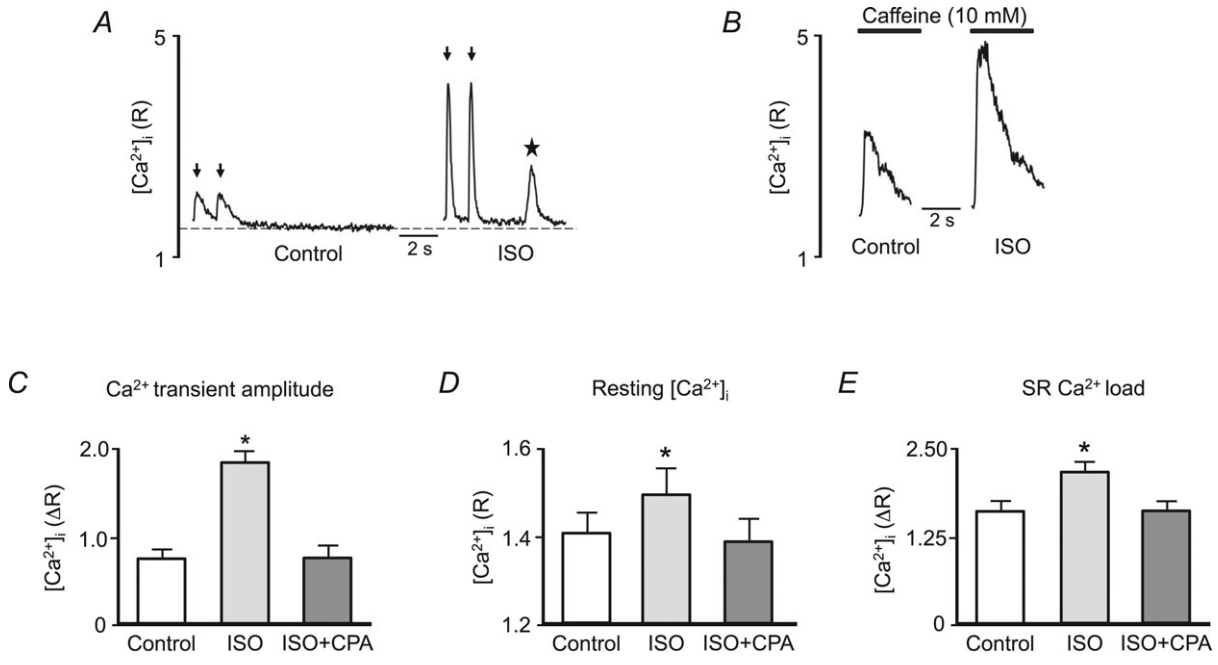

Figure 1. Effects of isoproterenol on intracellular Ca^{2+} handling
A, example cytosolic Ca^{2+} transients measured with indo-1 (0.75 Hz, electrical stimuli marked by arrows) followed by rest under control conditions ($[Ca^{2+}]_o = 2$ mM) and in the presence of 1 μM ISO. Control resting $[Ca^{2+}]_i$ level is marked by dashed line. Note spontaneous Ca^{2+} wave that occurred during the rest period in the presence of ISO (star). *B*, example $[Ca^{2+}]_i$ increases in response to 10 mM caffeine (black bars) used to assess SR Ca^{2+} content. Caffeine was applied immediately after identical 0.75 Hz pacing trains as shown in *A*, prior to the occurrence of spontaneous Ca^{2+} waves. Summary data of Ca^{2+} transient amplitude (0.75 Hz; *C*), resting $[Ca^{2+}]_i$ (*D*) and SR Ca^{2+} load (*E*) under control conditions, in the presence of ISO, and in the presence of ISO with 7.5 μM cyclopiazonic acid (CPA) in 100 μM $[Ca^{2+}]_o$. $^*P < 0.05$ *versus* control.

where waves occur. For this we designed experiments to observe Ca^{2+} waves under control conditions and to determine if, in the presence of ISO, Ca^{2+} waves were absent at the same $[Ca^{2+}]_{SR}$ level or would require even higher $[Ca^{2+}]_{SR}$ to occur. As spontaneous Ca^{2+} waves were not observed in normal $[Ca^{2+}]_o$ of 2 mM (Fig. 2*Ba* and *D*), $[Ca^{2+}]_o$ was raised to 7 mM and electrical stimulation frequency was incrementally increased to elevate $[Ca^{2+}]_{SR}$ (Fig. 3*B*) until Ca^{2+} waves were observed during rest from stimulation (see Methods for details on the stimulation–rest protocol). The highest near steady-state $[Ca^{2+}]_{SR}$ where Ca^{2+} waves were absent was defined as the control *no-wave* threshold (level 1 in Fig. 3*Aa*) while the lowest $[Ca^{2+}]_{SR}$ that associated with Ca^{2+} waves was defined as the control *wave* threshold (level 2 in Fig. 3*Ab*). Across all experiments ($n = 21$ cells), the stimulation frequencies associated with the *no-wave* and *wave* thresholds were 0.83 ± 0.05 and 0.93 ± 0.05 Hz, respectively. We then applied ISO to the same cell which increased $[Ca^{2+}]_{SR}$ due to its stimulatory effect on SERCA. As $[Ca^{2+}]_{SR}$ subsequently declined during an extended period of rest we determined the lowest $[Ca^{2+}]_{SR}$ that

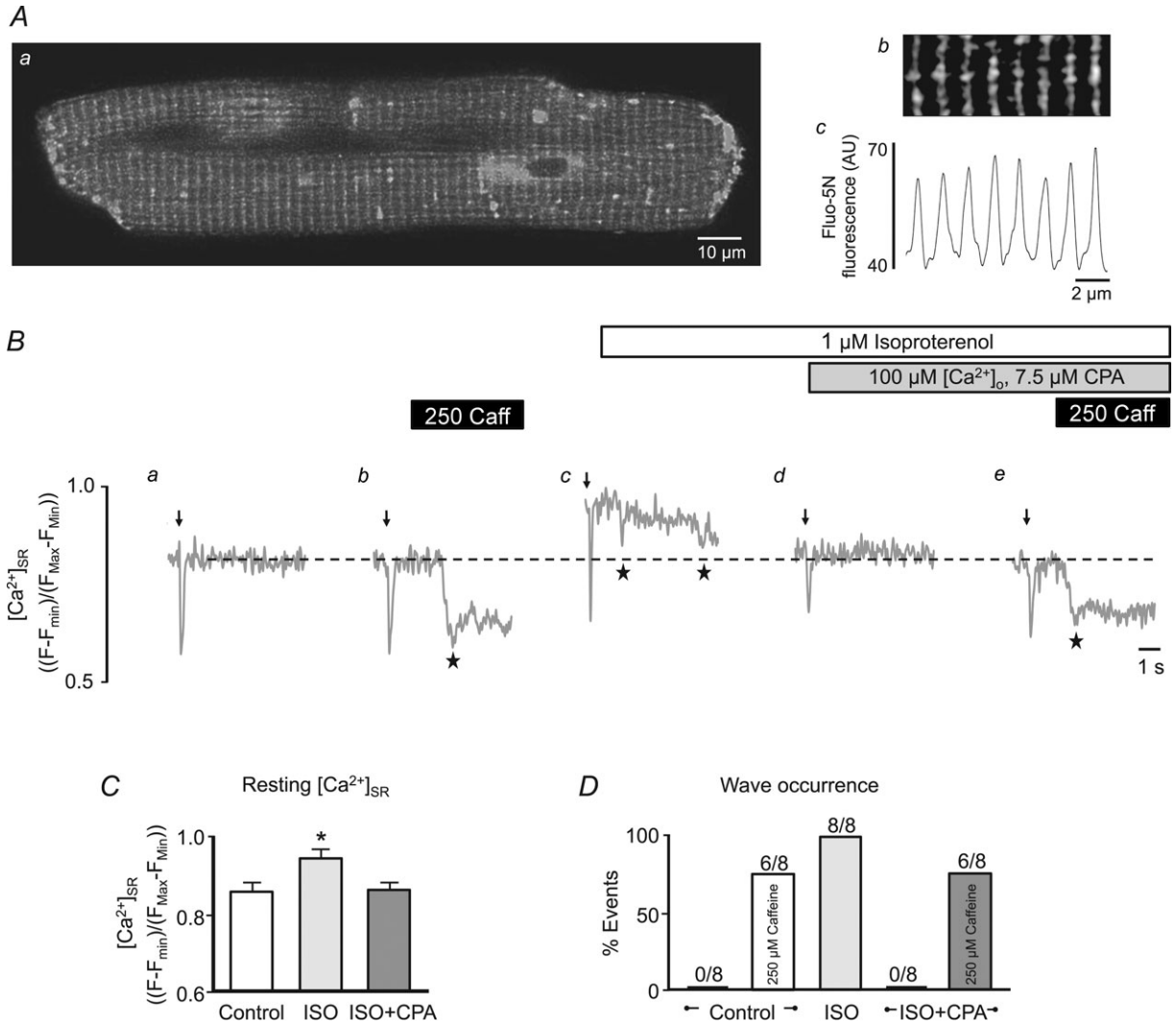

Figure 2. Direct $[Ca^{2+}]_{SR}$ measurements following isoproterenol application
A, confocal fluorescence image (a) of a myocyte with the SR loaded with the low-affinity Ca^{2+} indicator fluo-5N. Enlarged region of image (b) and corresponding fluorescence profile (c) showing patterning of the junctional SR network. AU, arbitrary units of fluo-5N fluorescence. *B*, example $[Ca^{2+}]_{SR}$ measurements with fluo-5N fluorescence showing an electrically induced Ca^{2+} depletion (arrow, 0.75 Hz) followed by rest under control conditions (*a* and *b*), in the presence of ISO (*c*) (*a*–*c*: $[Ca^{2+}]_o = 2$ mM), and in the presence of ISO with 7.5 μM CPA in 100 μM $[Ca^{2+}]_o$ (*d* and *e*). In traces *b* and *e* 250 μM caffeine (250 Caff) was applied to pharmacologically sensitize RyRs and induce Ca^{2+} waves. Ca^{2+} waves are visible in fluo-5N fluorescence profiles as a non-triggered decrease in fluorescence (stars). Summary data of resting $[Ca^{2+}]_{SR}$ (*C*) and Ca^{2+} wave occurrence (*D*) under the conditions shown in *B*. Ca^{2+} wave occurrence is presented as fraction (%) of cells showing waves, from a total of eight cells. $^*P < 0.05$.

preceded a Ca^{2+} wave (ISO wave threshold; level 3 in Fig. 3*Ac*). As shown in Fig. 3*A* (trace *c*), Ca^{2+} waves were frequent with ISO but were never observed at a $[Ca^{2+}]_{SR}$ below the control *no-wave* threshold (level 1), unless RyRs were sensitized with a low concentration of caffeine (250 μM).

We next supported these findings with a complementary experimental approach that allowed Ca^{2+} waves to be observed in a defined time interval (8 s) following rest from steady-state stimulation. For this the rest period where threshold levels were determined was preceded by a 30–60 s interval during which cells were electrically stimulated to establish identical steady-state conditions for the SR Ca^{2+} release mechanism. After control ($[Ca^{2+}]_o = 7$ mM) *no-wave* (level 1 in Fig. 4*Aa*) and *wave* (level 2 in Fig. 4*Ab*) thresholds were determined, ISO was applied for 5 min leading to an increase in $[Ca^{2+}]_{SR}$ and frequent Ca^{2+} waves (Fig. 4*Ac*). $[Ca^{2+}]_{SR}$ was then gradually reduced using application of ISO in the presence of low $[Ca^{2+}]_o$ (1 mM) and the SERCA inhibitor CPA (3 μM). In the example shown waves were no longer observed following rest from stimulation (Fig. 4*Ad*), unless RyRs were pharmacologically sensitized with 250 μM caffeine (Fig. 4*Ae*). Level 3 in Fig. 4*Ad* represents the *no-wave* threshold in the presence of ISO. Additional experiments were performed using the alternative SERCA inhibitor TG (1 μM) with similar results, and these results were pooled to provide the summary data shown in Fig. 4*B* and *C*. From 12 individual myocytes measurements of the *no-wave* and *wave* thresholds, as well as $[Ca^{2+}]_{SR}$ in the presence of ISO, followed by exposure to a SERCA blocker were obtained. In this set of experiments the *no-wave* threshold was 0.88 ± 0.01 $[(F - F_{Min})/(F_{Max} - F_{Min})]$ and the *wave* threshold was 0.90 ± 0.01 ($P < 0.05$, $n = 12$ cells, paired comparison). In the presence of ISO alone, all 12 cells exhibited Ca^{2+} waves, presumably due to the substantial increase of $[Ca^{2+}]_{SR}$ above the control threshold with $(F - F_{Min})/(F_{Max} - F_{Min})$ values approaching 1. Myocytes were subsequently exposed to ISO+CPA or ISO+TG for examination of the $[Ca^{2+}]_{SR}$ associated with waves (filled circles in Fig. 4*B*) or lack of waves (open circles). From each individual cell one or two measurements could be obtained for a total number of 18 experimental trials. In contrast to ISO alone, in the presence of ISO+CPA/TG waves were only observed in 8 of 18 experimental trials where $[Ca^{2+}]_{SR}$ was above the control *no-wave* threshold. The observation that in a majority of experimental trials waves were absent in the presence of ISO at $[Ca^{2+}]_{SR}$ levels where in control conditions waves were observed was indicative of an increase in the Ca^{2+} wave threshold. Quantitative analysis of the $[Ca^{2+}]_{SR}$ associated with the *no-wave* threshold under the respective conditions showed that this level was significantly higher in the presence of ISO+CPA/TG (Fig. 4*C*). The *no-wave* threshold under control conditions was at $[Ca^{2+}]_{SR} = 2.58 \pm 0.24$ mM ($n = 7$ cells) and increased to 3.39 ± 0.23 mM in the presence of ISO+CPA/TG ($n = 7$ cells; $P = 0.002$ *vs.* control). At $[Ca^{2+}]_{SR}$ below the control *no-wave* threshold, Ca^{2+} waves were not observed with ISO+CPA/TG (data not shown), unless RyRs were sensitized pharmacologically with 250 μM caffeine. In the presence of 250 μM caffeine Ca^{2+} waves were observed in all experimental trials (eight Ca^{2+} waves in eight cells) at a $[Ca^{2+}]_{SR}$ below the control *no-wave* threshold, indicative of a decrease in the Ca^{2+}

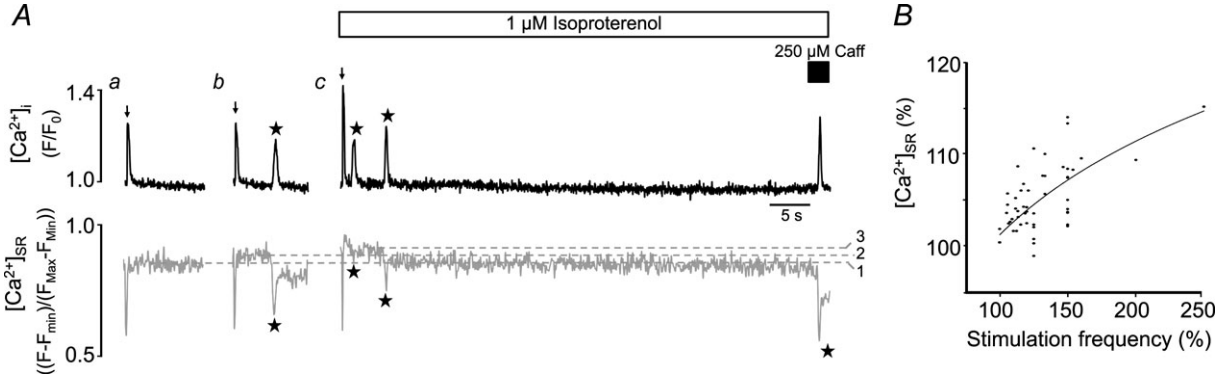

Figure 3. Ca^{2+} waves during sustained rest in the presence of isoproterenol
A, simultaneous $[Ca^{2+}]_i$ (rhod-2, upper traces in black) and $[Ca^{2+}]_{SR}$ (fluo-5N, lower traces in grey) measurements following rest from electrical stimulation under control conditions (7 mM $[Ca^{2+}]_o$, $a = 1.1$ Hz, $b = 1.3$ Hz) and in the presence of ISO (*c*: 2 mM $[Ca^{2+}]_o$, 1.3 Hz). Electrical stimulation frequency was incrementally increased to elevate $[Ca^{2+}]_{SR}$ and determine the threshold level for Ca^{2+} waves. In the example shown, Ca^{2+} waves were only observed when $[Ca^{2+}]_{SR}$ was higher than the control threshold level, unless RyRs were pharmacologically sensitized using 250 μM caffeine. Dashed lines: 1, *no-wave* threshold control; 2, *wave* threshold control; 3, *wave* threshold ISO. *B*, positive correlation between electrical stimulation frequency (range 0.5–1.3 Hz) and resting $[Ca^{2+}]_{SR}$ measured using fluo-5N fluorescence. Frequency and $[Ca^{2+}]_{SR}$ values are normalized to the respective values found at the lowest pacing frequency in each experimental trial.

wave threshold. Quantification of the *no-wave* threshold in the presence of 250 μM caffeine and ISO+CPA/TG showed that wave activity ceased when $[Ca^{2+}]_{SR}$ dropped to 1.00 ± 0.11 mM ($n = 5$ cells), a level that was significantly ($P < 0.001$) below the control and ISO+CPA/TG *no-wave* thresholds.

The direct and dynamic $[Ca^{2+}]_{SR}$ measurements clearly revealed an increase in the Ca^{2+} wave threshold during β-adrenergic stimulation. To further support these direct measurements we obtained additional measurements of the *no-wave* threshold in the presence of ISO+CPA using the amplitude of the $[Ca^{2+}]_i$ increase in response to 10 mM caffeine to estimate SR Ca^{2+} content.

Figure 5*A* shows original traces to determine control *no-wave* (level 1) and *wave* (level 2) thresholds, followed by the *no-wave* threshold in the presence of ISO+CPA (level 3). As shown in example traces of Fig. 5*A* and summary data of Fig. 5*B*, the SR Ca^{2+} content associated with the disappearance of Ca^{2+} waves with ISO+CPA (ISO *no-wave* threshold) was significantly higher than the *wave* threshold observed under control conditions. Importantly, resting $[Ca^{2+}]_i$ was similar under these experimental conditions

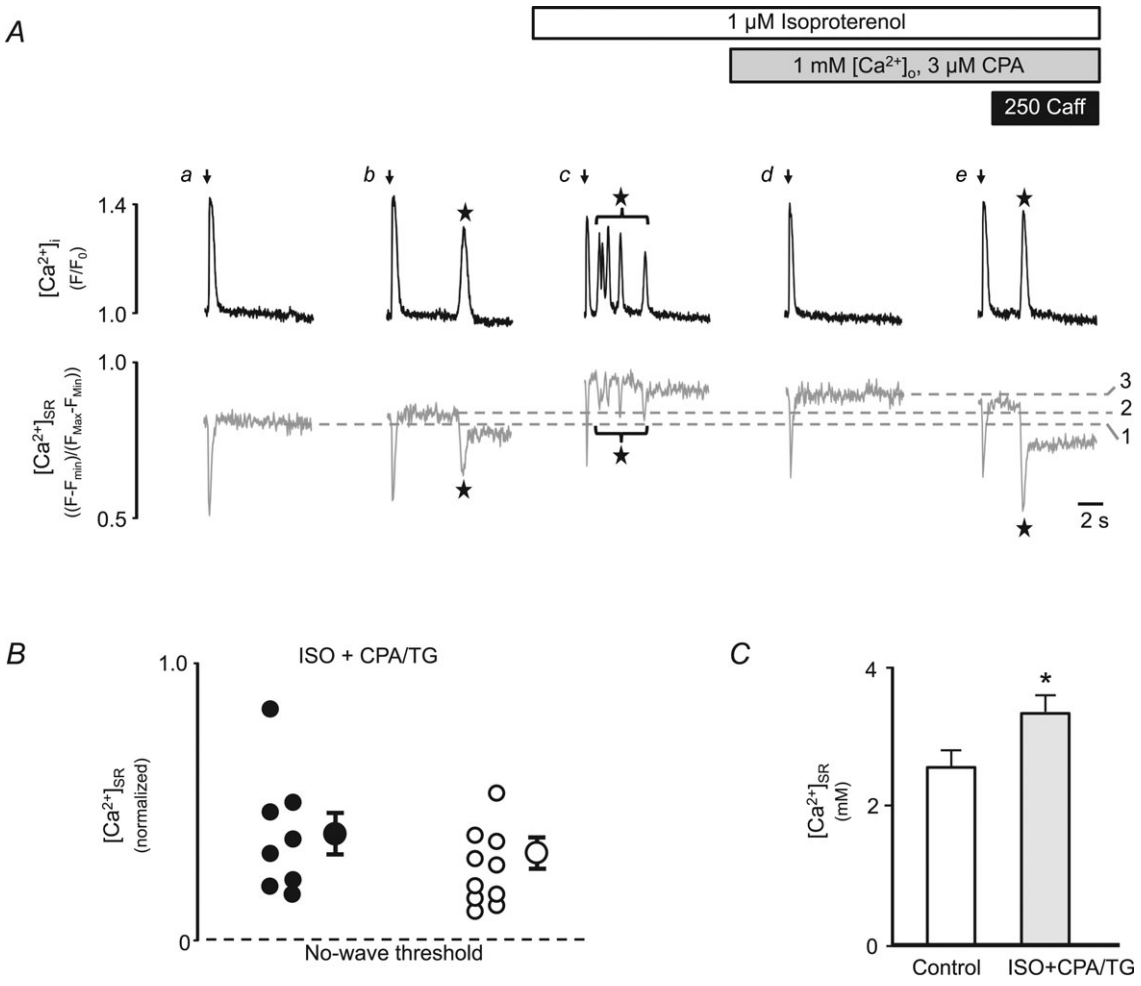

Figure 4. Isoproterenol increases the intra-SR Ca^{2+} wave threshold, determined by direct $[Ca^{2+}]_{SR}$ measurements
A, simultaneous $[Ca^{2+}]_i$ (rhod-2, upper traces in black) and $[Ca^{2+}]_{SR}$ (fluo-5N, lower traces in grey) measurements following rest from electrical stimulation (arrows) under control conditions (*a*: 7 mM $[Ca^{2+}]_o$, 0.7 Hz; *b:* 7 mM $[Ca^{2+}]_o$, 0.75 Hz), in the presence of ISO (*c*: 2 mM $[Ca^{2+}]_o$, 0.75 Hz) and in the presence of ISO with 3 μM CPA (*d* and *e*: 1 mM $[Ca^{2+}]_o$, 0.75 Hz). Dashed lines: 1, *no-wave*, threshold control; 2, *wave* threshold, control; 3, *no*-wave threshold, ISO. Subsequent application of 250 μM caffeine induced a Ca^{2+} wave (*e*). Waves are marked by stars. *B*, normalized $[Ca^{2+}]_{SR}$ values from 18 individual experimental trials (from 12 cells) in ISO+CPA/TG separated by the criteria whether waves were observed (filled circle) or not (open circles), together with the mean ± SEM of $[Ca^{2+}]_{SR}$ for the two groups. For each individual trial $[Ca^{2+}]_{SR}$ was normalized to the maximal fluorescence observed in the presence of 1 μM ISO ($[Ca^{2+}]_{SR,normalized} = 1$) and the *no-wave* threshold under control conditions ($[Ca^{2+}]_{SR,normalized} = 0$). *C*, quantification of the $[Ca^{2+}]_{SR}$ associated with the *no-wave* threshold under control conditions (open bar) and in the presence of ISO+CPA/TG (shaded bar). $^*P < 0.002$ *vs*. control, $n = 7$ cells.

(Fig. 5*C*; dotted line in Fig. 5*A*), which excluded the possibility that ISO-dependent changes in global cytosolic $[Ca^{2+}]_i$ were responsible for the observed effects on the wave threshold. Thus, the observed differences in SR Ca^{2+} content (Figs 4*A* and 5*B*) where waves occurred reflect a true increase in the intra-SR Ca^{2+} wave threshold.

Recent work has proposed that, in addition to the Ca^{2+} wave threshold, altered RyR 'refractoriness' may be a critical factor regulating SR Ca^{2+} release and the generation of Ca^{2+} waves (Ramay *et al.* 2011; Belevych *et al.* 2012). This concept is supported by direct measurements of $[Ca^{2+}]_{SR}$ which show that after $[Ca^{2+}]_{SR}$ recovers to a steady-state level following electrical stimulation a finite time interval (latency period) remains prior to Ca^{2+} wave initiation (Figs 2*B*, 3*A* and 4*A*; see also Domeier *et al.* 2010; Belevych *et al.* 2012; Maxwell *et al.* 2012). We therefore examined SR Ca^{2+} refilling, $[Ca^{2+}]_{SR}$ and wave latency in experiments where waves were observed. In these experiments two measurements of $[Ca^{2+}]_{SR}$, SR Ca^{2+} refilling times and Ca^{2+} wave latency were obtained from an individual cell (nine cells total), one at the *wave* threshold (Fig. 6*Aa*) and one after $[Ca^{2+}]_{SR}$ was increased above the control wave threshold (Fig. 6*Ab*). $[Ca^{2+}]_{SR}$ was increased by increasing the pacing frequency prior to the rest period during which Ca^{2+} waves were observed. Under control conditions SR Ca^{2+} refilling time (marked by dark grey area in Fig. 6*A*) was independent of initial $[Ca^{2+}]_{SR}$ (416 ± 25 ms at $[Ca^{2+}]_{SR} = 0.95 \pm 0.01$ $(F - F_{Min})/(F_{Max} - F_{Min})$, *versus* 416 ± 28 ms at $[Ca^{2+}]_{SR} = 0.91 \pm 0.01$; $n = 9$ cells). In the presence of ISO, SR Ca^{2+} refilling time was significantly shorter than under control conditions (227 ± 26 ms, $n = 6$ cells, $P < 0.001$ compared with control), and was slowed by subsequent SERCA inhibition with CPA or TG (367 ± 96 ms). The acceleration of SR refilling in the presence of ISO is explained by the stimulatory β-adrenergic effect on SERCA.

Analysis of wave latency revealed several interesting features. In control conditions (Fig. 6*B*; circles in Fig. 6*D*) as well as in the presence of ISO (Fig. 6*C*; squares in Fig. 6*D*), wave latency was highly dependent on $[Ca^{2+}]_{SR}$, with higher $[Ca^{2+}]_{SR}$ leading to a significantly shorter wave latency. Furthermore, in the presence of ISO the dependence of wave latency on $[Ca^{2+}]_{SR}$ shifted towards

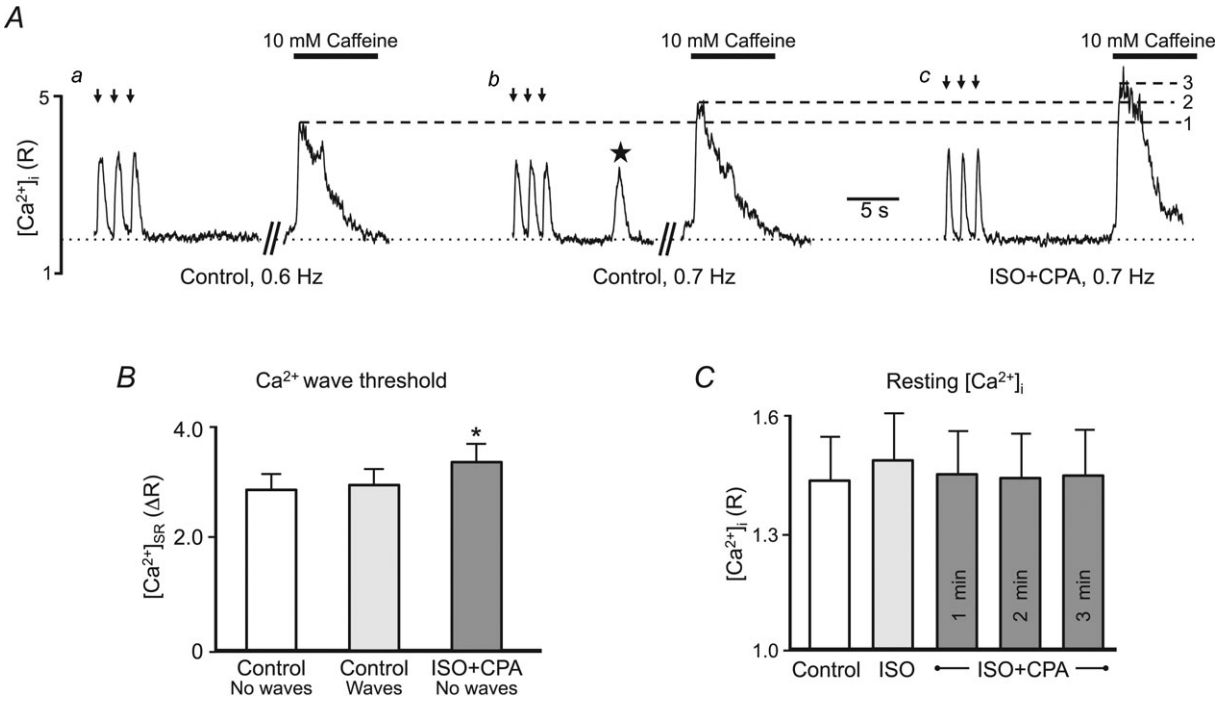

Figure 5. Isoproterenol increases the intra-SR Ca^{2+} wave threshold determined by cytosolic $[Ca^{2+}]_i$ measurements
A, example indo-1 $[Ca^{2+}]_i$ measurements following rest from electrical stimulation (arrows) under control conditions (7 mM $[Ca^{2+}]_o$, $a = 0.6$ Hz, $b = 0.7$ Hz) and in the presence of ISO with 3 μM CPA (*c*: 1 mM $[Ca^{2+}]_o$, 0.7 Hz). Caffeine (10 mM) was applied after rest from a separate pacing train to assess SR Ca^{2+} content at each pacing frequency under control conditions and to determine *no-wave* (dashed line 1) and *wave* (dashed line 2) threshold SR Ca^{2+} content. In the presence of ISO+CPA, when waves were not observed following rest from pacing, 10 mM caffeine was applied to assess the *no-wave* threshold in ISO (dashed line 3). Star denotes Ca^{2+} wave. Dotted line: resting $[Ca^{2+}]_i$. *B*, summary data of SR Ca^{2+} content under the conditions shown in *A* ($n = 8$ cells). *C*, average resting $[Ca^{2+}]_i$ was similar under these experimental conditions ($n = 7$ cells). $^*P < 0.05$.

longer latencies, i.e. for a given SR Ca^{2+} content, the wave latency was prolonged in the presence of ISO compared with control conditions. For example, despite the fact during ISO treatment $[Ca^{2+}]_{SR}$ was significantly higher than under control conditions [ISO (grey square) 1.0 ± 0 *vs.* control (grey circle) 0.95 ± 0.01; $P < 0.001$], latency times were similar (ISO 1.02 ± 0.22 s *vs.* control 1.44 ± 0.27 s; not significantly different at $P = 0.38$). Furthermore, comparison of control conditions (Fig. 6*D*, grey circle) with ISO+CPA/TG treatment (Fig. 6*D*, black square) showed that at a similar $[Ca^{2+}]_{SR}$ (control 0.95 ± 0.01 *vs.* ISO+CPA 0.93 ± 0.02; not significantly different at $P = 0.28$) latency times were significantly shorter under control conditions (control 1.44 ± 0.27 s *vs.* ISO+CPA/TG 4.42 ± 0.85 s; $P < 0.01$).

In summary, our study shows that during β-adrenergic stimulation the propensity for Ca^{2+} waves is increased because of significantly increased $[Ca^{2+}]_{SR}$ and SR Ca^{2+} overload. Counteracting the increase in $[Ca^{2+}]_{SR}$ are changes in two $[Ca^{2+}]_{SR}$-dependent parameters, with an increase in Ca^{2+} wave threshold and a prolonged wave latency.

Discussion

During sympathetic nervous system activation the heart experiences chronotropic, inotropic and lusitropic effects that act in concert to facilitate an increase in cardiac output. At the level of the individual cardiomyocyte catecholamine binding to β-adrenoceptors causes an increase in cellular Ca^{2+} cycling that associates with Ca^{2+} waves, suggesting an acute lowering of the intra-SR Ca^{2+} wave threshold. However, our data using direct, dynamic measurements of this threshold clearly show that to the contrary, the threshold for Ca^{2+} waves is *increased* by acute β-adrenergic stimulation. The direct $[Ca^{2+}]_{SR}$ measurements presented here support recent quantification of the Ca^{2+} wave threshold in mouse ventricular myocytes which show a similar effect of the Ca^{2+} wave threshold increasing following acute β-adrenergic stimulation (Kashimura *et al.* 2010; Stokke *et al.* 2010*a*).

The Ca^{2+} wave threshold is a useful experimental parameter that has greatly advanced our understanding of the mechanisms of cardiac arrhythmia, including those associated with diseases such as CPVT and

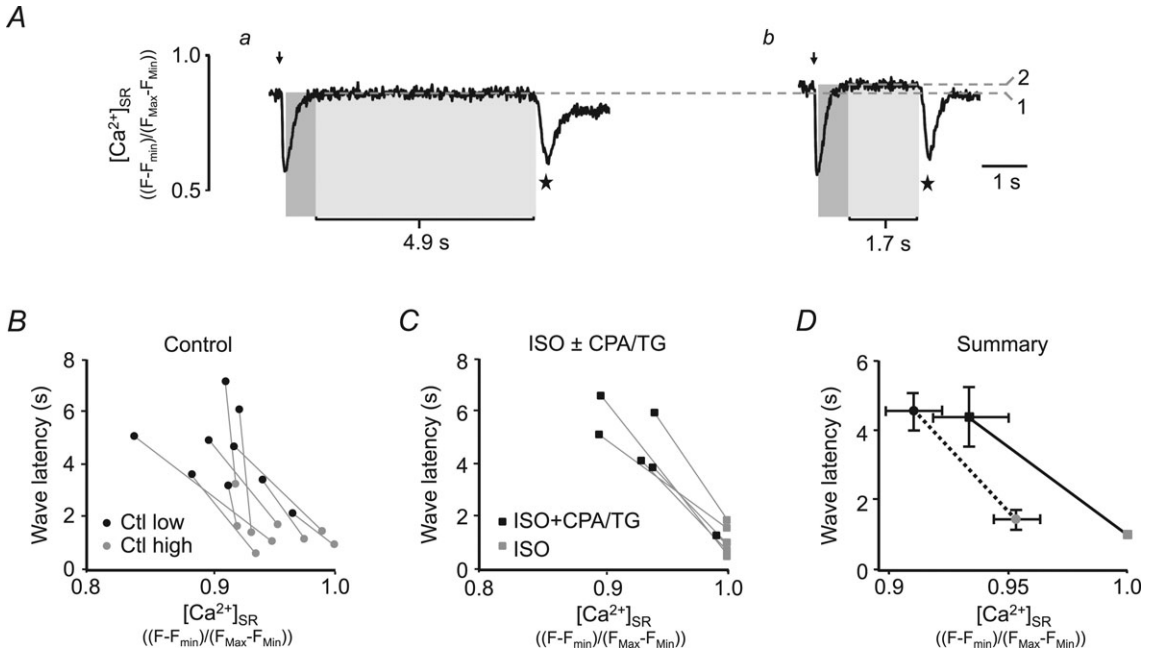

Figure 6. Wave latency is highly dependent on $[Ca^{2+}]_{SR}$
A, representative fluo-5N fluorescence traces from a cell with $[Ca^{2+}]_{SR}$ at the wave threshold (*a*, threshold marked with dashed line 1) and above the wave threshold (*b*, steady-state $[Ca^{2+}]_{SR}$ before wave marked with dashed line 2). In each trace, arrow denotes AP stimulation triggering $[Ca^{2+}]_{SR}$ depletion, followed by SR Ca^{2+} refilling (dark grey) and a wave latency time (light grey) prior to the Ca^{2+} wave (marked by star). *B*, individual paired experiments obtained from nine cells, each yielding a wave latency measurement at two different $[Ca^{2+}]_{SR}$ levels under control conditions (Ctl low, Ctl high). *C*, individual paired experiments obtained from six cells, each yielding a wave latency measurement in the presence of ISO (grey square) alone and in the combined presence of ISO plus CPA or TG (ISO+CPA/TG black square). *D*, summary data (averages from data shown in *B* and *C*) of the relationship between $[Ca^{2+}]_{SR}$ and Ca^{2+} wave latency under control conditions at two different $[Ca^{2+}]_{SR}$ levels (circles), in ISO (grey square) and in ISO+CPA/TG (black square). Statistical significance analysis of these data is presented in the text.

heart failure. Experimental evidence and computational modelling implicate numerous intracellular factors in Ca^{2+} wave generation and propagation, including RyR open probability, release junction (sarcomere) spacing, SR Ca^{2+} uptake via SERCA, and cytosolic and intra-SR Ca^{2+} buffering processes (Izu *et al.* 2006; Ramay *et al.* 2010; Swietach *et al.* 2010). The appearance of Ca^{2+} waves as $[Ca^{2+}]_{SR}$ increases can be explained by well-established RyR gating mechanisms, most notably that the RyR open probability increases at high $[Ca^{2+}]_{SR}$ due to the channel's inherent sensitivity to $[Ca^{2+}]_{SR}$ (Gyorke & Gyorke, 1998; Fill & Copello, 2002). Furthermore, because Ca^{2+} release terminates at a set level of $[Ca^{2+}]_{SR}$ (Zima *et al.* 2008) Ca^{2+} sparks will be high-amplitude release events at high $[Ca^{2+}]_{SR}$, which will increase the ability of Ca^{2+} released during a spark to overcome cytosolic buffering and diffuse to adjacent release junctions and trigger CICR. These properties result in the appearance of Ca^{2+} waves at a defined $[Ca^{2+}]_{SR}$ (the wave threshold), and make the time to wave initiation highly dependent on $[Ca^{2+}]_{SR}$ (Fig. 6).

Direct measurements of $[Ca^{2+}]_{SR}$ (Fig. 6) illustrate that Ca^{2+} waves do not occur immediately after $[Ca^{2+}]_{SR}$ reaches a steady-state concentration (Domeier *et al.* 2010; Belevych *et al.* 2012; Maxwell *et al.* 2012) and therefore a time-dependent 'refractory' component of wave generation exists (Belevych *et al.* 2012). While this appears to conceptually challenge the Ca^{2+} wave threshold as being the critical parameter that determines whether a Ca^{2+} wave will be observed, our data suggest that changes in wave refractory (latency) time may simply be a manifestation of how high $[Ca^{2+}]_{SR}$ is above the Ca^{2+} wave threshold. In an individual cell the Ca^{2+} wave threshold was highly reproducible among experimental trials, yet different wave latency times were recorded depending on $[Ca^{2+}]_{SR}$, with shorter times observed *above* the wave threshold than *at* the wave threshold (Fig. 6*B*). This relationship was similarly observed in canine ventricular myocytes (Belevych *et al.* 2012). Based on these data our working model (Fig. 7) is that the cell has a distinct intra-luminal $[Ca^{2+}]_{SR}$ threshold for Ca^{2+} wave development (Díaz *et al.* 1997*b*; Jiang *et al.* 2004; Venetucci *et al.* 2007). At $[Ca^{2+}]_{SR}$ below this threshold the probability for wave development following rest from steady-state stimulation is low and thus the cell has a wave latency period that approaches infinity (Fig. 7*a*). When $[Ca^{2+}]_{SR}$ reaches the Ca^{2+} wave threshold the probability that a Ca^{2+} wave will occur increases, yet due to the stochastic nature of Ca^{2+} wave initiation there will be a finite latency period associated with the wave (Fig. 7*b*). As $[Ca^{2+}]_{SR}$ continues to increase above this distinct wave threshold, the Ca^{2+} wave probability remains high but now the latency period will be shortened due to the stimulatory effect of luminal $[Ca^{2+}]_{SR}$ on RyR open probability, increasing the likelihood of a spontaneous release event to trigger a Ca wave (Fig. 7*c*) (Gyorke & Gyorke, 1998). During β-adrenergic stimulation, despite the observation that the wave threshold is increased, the massive gain of Ca^{2+} in the SR results in a further shortening of the latency period (Fig. 7*f*). Overall, the latency period is inversely proportional (Fig. 6*D*) to the degree by which $[Ca^{2+}]_{SR}$ exceeds the wave threshold. For a given $[Ca^{2+}]_{SR}$ level, however, the latency period is longer in the presence of ISO (Fig. 7*d*) than under control conditions (Fig. 7*c*), and is similar when $[Ca^{2+}]_{SR}$ exceeds the respective wave thresholds to the same degree (Fig. 7*c* *vs.* Fig. 7*e*). Thus, there may be an important distinction between the parameter of the Ca^{2+} wave threshold and that of the wave latency period. A cell may have multiple latency periods depending on how high $[Ca^{2+}]_{SR}$ is above a distinct wave threshold (Fig. 6), and thus the wave threshold measurement is a more biophysically accurate way to assess the ability of the SR to sequester (or spontaneously release) Ca^{2+}. Alternatively, however, the wave latency period may be the most physiologically relevant way to describe diastolic Ca^{2+} waves with respect to cellular SR Ca^{2+} content (i.e. inotropic state of heart) and rate of AP stimulation (i.e. chronotropic state of the heart). *In vivo* these complex relationships will determine if an arrhythmogenic Ca^{2+} wave will be observed during diastole in the beating heart.

β-Adrenergic modulation of the RyR and Ca^{2+} waves

Alterations in RyR activity (e.g. via phosphorylation or redox modification) will lead to subsequent changes in the intra-SR Ca^{2+} wave threshold, as shown by RyR inhibitors (Overend *et al.* 1997) or activators (Venetucci *et al.* 2007; Kong *et al.* 2008) raising or lowering the threshold, respectively. The signalling events that regulate RyR activity downstream of β-adrenergic stimulation remain highly contentious, with conflicting reports throughout the literature (for example see commentaries by Yamaguchi & Meissner, 2007; Houser, 2010; Bers, 2012). Most investigations, however, report an increase in RyR activity which would result in a decrease in the Ca^{2+} wave threshold. The observation of an increased Ca^{2+} wave threshold is therefore counterintuitive. Discrepant results may emerge due to the multiple assays of RyR function which may not be mechanistically equivalent, particularly following activation of complex cellular signalling pathways (reviewed by George, 2008). As an example, systolic Ca^{2+} release in response to the AP, representing activation of RyRs via cytosolic Ca^{2+}, may exhibit distinct regulation when compared to diastolic Ca^{2+} release triggered by SR Ca^{2+} overload and activation of RyRs by $[Ca^{2+}]_{SR}$. The properties of local diastolic Ca^{2+} release events (Ca^{2+} spark frequency, Ca^{2+} spark amplitude, non-spark-mediated SR Ca^{2+} leak) may also

be differentially modulated (Zhou *et al.* 2009) and subsequently alter the ability of Ca^{2+} waves to initiate and propagate. Recently, novel genetic approaches have been utilized to ablate (Wehrens *et al.* 2006; Benkusky *et al.* 2007; Chelu *et al.* 2009) or chronically activate (Shan *et al.* 2010; van Oort *et al.* 2010) RyR phosphorylation sites *in vivo*, and gain additional insight into RyR regulation that may occur downstream of β-adrenergic signalling. However, this strategy may result in a cellular phenotype that is distinct from that observed when all cellular effectors are activated in parallel following receptor activation. Complex signal integration at the level of the RyR is expected given the multiple regulatory sites on the channel protein and the role of the macromolecular RyR complex as a subcellular signalling platform.

β-Adrenergic modulation of SERCA and Ca^{2+} waves

Although the Ca^{2+} wave threshold is primarily set by the regulation of RyR release channels, it is likely further tuned by altering the function of additional cellular proteins involved in wave generation. One of the main effects of β-adrenergic stimulation is to increase SERCA activity, which is accomplished via phosphorylation of the SERCA inhibitory protein phospholamban. Phospholamban phosphorylation, principally by protein kinase A although there is some evidence for a role of Ca^{2+}/calmodulin-dependent protein kinase II, reduces its inhibitory interactions with SERCA and leads to a dramatic increase in SERCA activity and $[Ca^{2+}]_{SR}$. Indeed, SERCA-mediated Ca^{2+} uptake increasing $[Ca^{2+}]_{SR}$ above the intra-SR Ca^{2+} wave threshold is one of the principal

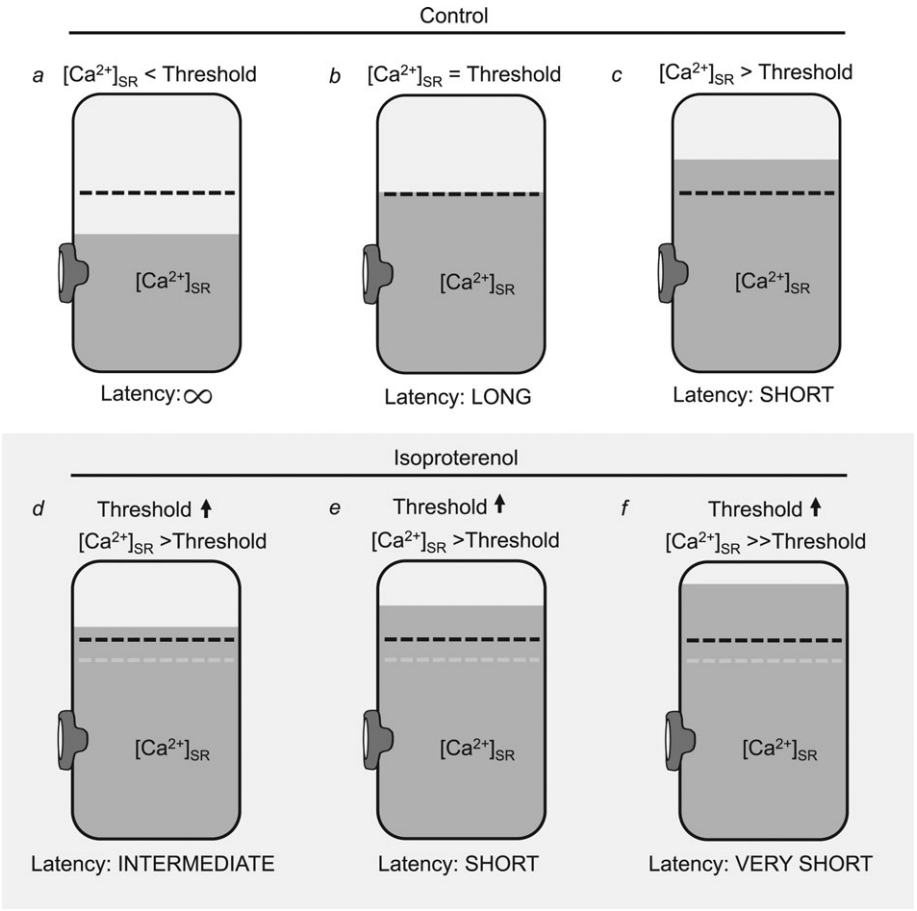

Figure 7. Schematic diagram of proposed relationship between SR Ca^{2+} content, Ca^{2+} wave threshold and latency
Schematic diagram of the SR showing the relationship between $[Ca^{2+}]_{SR}$ (shaded area), the Ca^{2+} wave threshold (dashed black line) and Ca^{2+} wave latency when $[Ca^{2+}]_{SR}$ is below (*a*), at (*b*) and above (*c*) the Ca^{2+} wave threshold. In the presence of ISO (*d*, *e* and *f*) the Ca^{2+} wave threshold (dashed black line) is increased when compared with control conditions (dashed grey line). When $[Ca^{2+}]_{SR}$ is similar between control condition (*c*) and ISO condition (*d*), latency is shorter in control due to $[Ca^{2+}]_{SR}$ being higher above the respective wave threshold. When $[Ca^{2+}]_{SR}$ is elevated by the same relative amount above the wave threshold under control conditions (*c*) and with ISO (*e*) wave latencies are similar even though the total $[Ca^{2+}]_{SR}$ is higher with ISO. Under most experimental conditions $[Ca^{2+}]_{SR}$ increases dramatically in the presence of ISO, thus elevating $[Ca^{2+}]_{SR}$ well above the respective Ca^{2+} wave threshold, resulting in a very short wave latency (*f*).

mechanisms by which β-adrenergic stimulation increases Ca^{2+} wave probability, and is supported by data showing that genetic ablation of phospholamban dramatically increases the propensity of Ca^{2+} waves (Huser *et al.* 1998). SERCA activity may also directly contribute to Ca^{2+} wave propagation and thus, in part, determine the intra-SR Ca^{2+} wave threshold. It has been shown experimentally that SERCA inhibition increases Ca^{2+} wave velocity (Lukyanenko *et al.* 1999), and computer simulations predict that increasing SERCA activity prevents Ca^{2+} wave propagation by decreasing $[Ca^{2+}]_i$ and the ability of Ca^{2+} to diffuse between Ca^{2+} release junctions (Ramay *et al.* 2010). However, this cytosolic Ca^{2+} buffering effect may be countered by the ability of SERCA to locally increase $[Ca^{2+}]_{SR}$ and create intra-SR 'Ca^{2+} sensitization' wavefronts which precede the cytosolic Ca^{2+} wave (Keller *et al.* 2007; Maxwell & Blatter, 2012). This provocative model is based on experimental evidence contradictory to that of Lukyanenko *et al.* (1999), which shows that SERCA inhibition decreases Ca^{2+} wave velocity (Keller *et al.* 2007). While this model of wave propagation can be reproduced by computer simulations (Ramay *et al.* 2010), it is critically dependent on the speed by which Ca^{2+} diffuses within the SR network, which is difficult to determine empirically and remains controversial (Swietach *et al.* 2008; Picht *et al.* 2011). Electrophysiological measurement of the Ca^{2+} wave threshold in rat myocytes showed that SERCA inhibition decreased the intra-SR Ca^{2+} wave threshold (O'Neill *et al.* 2004), and these data are supported by studies of transgenic mice with reduced SERCA abundance that also have a decreased Ca^{2+} wave threshold, although interpretation of data from this model may be complicated by concomitant compensatory changes in RyR function (Stokke *et al.* 2010*a*,*b*). However, in mouse ventricular myocytes where the Ca^{2+} wave threshold was increased following β-adrenergic stimulation, the Ca^{2+} wave threshold did not appear to correlate with SERCA activity (Kashimura *et al.* 2010), and it remains unclear if the increase in SERCA activity that accompanies β-adrenergic stimulation plays a role in increasing the intra-SR Ca^{2+} wave threshold.

β-Adrenergic modulation of cellular buffering and Ca^{2+} waves

As predicted by mathematical models, changes in the buffering properties of the cytosol and/or SR would also alter Ca^{2+} wave propagation and the intra-SR Ca^{2+} wave threshold. β-Adrenoceptor activation leads to a decrease in myofilament Ca^{2+} sensitivity which is believed in part to underlie the lusitropic effect of catecholamines on the heart. This change will likely lead to altered Ca^{2+} buffering properties and Ca^{2+} transport kinetics, although it remains unclear if these changes alter Ca^{2+} wave propagation. Recent evidence suggests that increased Ca^{2+} sensitivity promotes arrhythmogenesis, leading to the hypothesis that increased myofilament Ca^{2+} affinity may augment Ca^{2+} wave propagation by altering diastolic contracture and shortening the distance between release clusters (Izu *et al.* 2006; Chen-Izu *et al.* 2007). Changes in intra-SR Ca^{2+} buffering properties have also been shown to affect Ca^{2+} wave propagation (Kubalova *et al.* 2004). While there is experimental evidence that the intra-SR Ca^{2+} binding protein calsequestrin may be regulated by phosphorylation (Cala & Jones, 1991), and that phosphorylation increases Ca^{2+} binding capacity of calsequestrin (Beard *et al.* 2008), it is unclear if this phosphorylation occurs in response to acute activation of intracellular signalling pathways. Furthermore, the addition of exogenous intra-SR Ca^{2+} buffers alters Ca^{2+} wave frequency and amplitude without changing the intra-SR Ca^{2+} wave threshold (Kubalova *et al.* 2004), and thus it is unlikely that the acute effect of β-adrenergic stimulation on the intra-SR Ca^{2+} wave threshold is due to changes in intra-SR Ca^{2+} binding protein function.

Summary

β-Adrenergic stimulation enhances intracellular Ca^{2+} cycling and increases SR Ca^{2+} load to the extent that spontaneous and potentially detrimental Ca^{2+} waves occur. As shown in this study the β-adrenoceptor-mediated increase in SR Ca^{2+} load is also accompanied by an increase of the intra-SR Ca^{2+} wave threshold and a prolongation of the wave latency period. These two factors may be interpreted as a protective mechanism against diastolic arrhythmogenic Ca^{2+} release in the heart.

References

Beard NA, Wei L, Cheung SN, Kimura T, Varsanyi M & Dulhunty AF (2008). Phosphorylation of skeletal muscle calsequestrin enhances its Ca^{2+} binding capacity and promotes its association with junctin. *Cell Calcium* **44**, 363–373.

Belevych AE, Terentyev D, Terentyeva R, Ho HT, Gyorke I, Bonilla IM, Carnes CA, Billman GE & Gyorke S (2012). Shortened Ca^{2+} signalling refractoriness underlies cellular arrhythmogenesis in a postinfarction model of sudden cardiac death. *Circ Res* **110**, 569–577.

Benkusky NA, Weber CS, Scherman JA, Farrell EF, Hacker TA, John MC, Powers PA & Valdivia HH (2007). Intact β-adrenergic response and unmodified progression toward heart failure in mice with genetic ablation of a major protein kinase A phosphorylation site in the cardiac ryanodine receptor. *Circ Res* **101**, 819–829.

Bers DM (2012). Ryanodine receptor S2808 phosphorylation in heart failure: smoking gun or red herring. *Circ Res* **110**, 796–799.

Bovo E, Lipsius SL & Zima AV (2012). Reactive oxygen species contribute to the development of arrhythmogenic Ca^{2+} waves during β-adrenergic receptor stimulation in rabbit cardiomyocytes. *J Physiol* **590**, 3291–3304.

Cala SE & Jones LR (1991). Phosphorylation of cardiac and skeletal muscle calsequestrin isoforms by casein kinase II. Demonstration of a cluster of unique rapidly phosphorylated sites in cardiac calsequestrin. *J Biol Chem* **266**, 391–398.

Capogrossi MC, Houser SR, Bahinski A & Lakatta EG (1987). Synchronous occurrence of spontaneous localized calcium release from the sarcoplasmic reticulum generates action potentials in rat cardiac ventricular myocytes at normal resting membrane potential. *Circ Res* **61**, 498–503.

Chelu MG, Sarma S, Sood S, Wang S, van Oort RJ, Skapura DG, Li N, Santonastasi M, Muller FU, Schmitz W, Schotten U, Anderson ME, Valderrabano M, Dobrev D & Wehrens XH (2009). Calmodulin kinase II-mediated sarcoplasmic reticulum Ca^{2+} leak promotes atrial fibrillation in mice. *J Clin Invest* **119**, 1940–1951.

Chen-Izu Y, Ward CW, Stark W Jr, Banyasz T, Sumandea MP, Balke CW, Izu LT & Wehrens XH (2007). Phosphorylation of RyR_2 and shortening of RyR_2 cluster spacing in spontaneously hypertensive rat with heart failure. *Am J Physiol Heart Circ Physiol* **293**, H2409–2417.

Curran J, Brown KH, Santiago DJ, Pogwizd S, Bers DM & Shannon TR (2010). Spontaneous Ca waves in ventricular myocytes from failing hearts depend on Ca^{2+}-calmodulin-dependent protein kinase II. *J Mol Cell Cardiol* **49**, 25–32.

Curran J, Hinton MJ, Rios E, Bers DM & Shannon TR (2007). β-Adrenergic enhancement of sarcoplasmic reticulum calcium leak in cardiac myocytes is mediated by calcium/calmodulin-dependent protein kinase. *Circ Res* **100**, 391–398.

Díaz ME, Trafford AW, O'Neill SC & Eisner DA (1997*a*). A measurable reduction of s.r. Ca content follows spontaneous Ca release in rat ventricular myocytes. *Pflugers Arch* **434**, 852–854.

Díaz ME, Trafford AW, O'Neill SC & Eisner DA (1997*b*). Measurement of sarcoplasmic reticulum Ca^{2+} content and sarcolemmal Ca^{2+} fluxes in isolated rat ventricular myocytes during spontaneous Ca^{2+} release. *J Physiol* **501**, 3–16.

Domeier TL & Blatter LA (2010). Mechanisms of spontaneous calcium wave generation during β-adrenergic stimulation in rabbit ventricular myocytes. *Biophys J* **98**, 105a.

Domeier TL, Blatter LA & Zima AV (2010). Changes in intra-luminal calcium during spontaneous calcium waves following sensitization of ryanodine receptor channels. *Channels* **4**, 87–92.

Domeier TL, Maxwell JT & Blatter LA (2011). β-Adrenergic stimulation increases the intra-sarcoplasmic reticulum Ca threshold for spontaneous Ca waves. *Biophys J* **100**, 559a.

Drummond GB (2009). Reporting ethical matters in the *Journal of Physiology*: standards and advice. *J Physiol* **587**, 713–719.

Fedida D, Noble D, Rankin AC & Spindler AJ (1987). The arrhythmogenic transient inward current iTI and related contraction in isolated guinea-pig ventricular myocytes. *J Physiol* **392**, 523–542.

Fill M & Copello JA (2002). Ryanodine receptor calcium release channels. *Physiol Rev* **82**, 893–922.

Fujiwara K, Tanaka H, Mani H, Nakagami T & Takamatsu T (2008). Burst emergence of intracellular Ca^{2+} waves evokes arrhythmogenic oscillatory depolarization via the Na^+–Ca^{2+} exchanger: simultaneous confocal recording of membrane potential and intracellular Ca^{2+} in the heart. *Circ Res* **103**, 509–518.

George CH (2008). Sarcoplasmic reticulum Ca^{2+} leak in heart failure: mere observation or functional relevance? *Cardiovasc Res* **77**, 302–314.

Guo T, Zhang T, Mestril R & Bers DM (2006). Ca^{2+}/calmodulin-dependent protein kinase II phosphorylation of ryanodine receptor does affect calcium sparks in mouse ventricular myocytes. *Circ Res* **99**, 398–406.

Gyorke I & Gyorke S (1998). Regulation of the cardiac ryanodine receptor channel by luminal Ca^{2+} involves luminal Ca^{2+} sensing sites. *Biophys J* **75**, 2801–2810.

Houser SR (2010). Does protein kinase A-mediated phosphorylation of the cardiac ryanodine receptor play any role in adrenergic regulation of calcium handling in health and disease? *Circ Res* **106**, 1672–1674.

Huser J, Bers DM & Blatter LA (1998). Subcellular properties of $[Ca^{2+}]_i$ transients in phospholamban-deficient mouse ventricular cells. *Am J Physiol Heart Circ Physiol* **274**, H1800–1811.

Izu LT, Means SA, Shadid JN, Chen-Izu Y & Balke CW (2006). Interplay of ryanodine receptor distribution and calcium dynamics. *Biophys J* **91**, 95–112.

Jiang D, Xiao B, Yang D, Wang R, Choi P, Zhang L, Cheng H & Chen SR (2004). RyR2 mutations linked to ventricular tachycardia and sudden death reduce the threshold for store-overload-induced Ca^{2+} release (SOICR). *Proc Natl Acad Sci U S A* **101**, 13062–13067.

Kashimura T, Briston SJ, Trafford AW, Napolitano C, Priori SG, Eisner DA & Venetucci LA (2010). In the RyR2(R4496C) mouse model of CPVT, β-adrenergic stimulation induces Ca waves by increasing SR Ca content and not by decreasing the threshold for Ca waves. *Circ Res* **107**, 1483–1489.

Kass RS, Lederer WJ, Tsien RW & Weingart R (1978). Role of calcium ions in transient inward currents and aftercontractions induced by strophanthidin in cardiac Purkinje fibres. *J Physiol* **281**, 187–208.

Keller M, Kao JP, Egger M & Niggli E (2007). Calcium waves driven by "sensitization" wave-fronts. *Cardiovasc Res* **74**, 39–45.

Kong H, Jones PP, Koop A, Zhang L, Duff HJ & Chen SR (2008). Caffeine induces Ca^{2+} release by reducing the threshold for luminal Ca^{2+} activation of the ryanodine receptor. *Biochem J* **414**, 441–452.

Kranias EG & Solaro RJ (1982). Phosphorylation of troponin I and phospholamban during catecholamine stimulation of rabbit heart. *Nature* **298**, 182–184.

Kubalova Z, Gyorke I, Terentyeva R, Viatchenko-Karpinski S, Terentyev D, Williams SC & Gyorke S (2004). Modulation of cytosolic and intra-sarcoplasmic reticulum calcium waves by calsequestrin in rat cardiac myocytes. *J Physiol* **561**, 515–524.

Lindemann JP, Jones LR, Hathaway DR, Henry BG & Watanabe AM (1983). β-Adrenergic stimulation of phospholamban phosphorylation and Ca^{2+}-ATPase activity in guinea pig ventricles. *J Biol Chem* **258**, 464–471.

Lukyanenko V, Subramanian S, Gyorke I, Wiesner TF & Gyorke S (1999). The role of luminal Ca^{2+} in the generation of Ca^{2+} waves in rat ventricular myocytes. *J Physiol* **518**, 173–186.

Maxwell JT & Blatter LA (2012). Facilitation of cytosolic calcium wave propagation by local calcium uptake into the sarcoplasmic reticulum in cardiac myocytes. *J Physiol* **590**, 6037–6045.

Maxwell JT, Domeier TL & Blatter LA (2012). Dantrolene prevents arrhythmogenic Ca^{2+} release in heart failure. *Am J Physiol Heart Circ Physiol* **302**, H953–963.

O'Neill SC, Miller L, Hinch R & Eisner DA (2004). Interplay between SERCA and sarcolemmal Ca^{2+} efflux pathways controls spontaneous release of Ca^{2+} from the sarcoplasmic reticulum in rat ventricular myocytes. *J Physiol* **559**, 121–128.

Ogrodnik J & Niggli E (2010). Increased Ca^{2+} leak and spatiotemporal coherence of Ca^{2+} release in cardiomyocytes during β-adrenergic stimulation. *J Physiol* **588**, 225–242.

Overend CL, Eisner DA & O'Neill SC (1997). The effect of tetracaine on spontaneous Ca^{2+} release and sarcoplasmic reticulum calcium content in rat ventricular myocytes. *J Physiol* **502**, 471–479.

Picht E, Zima AV, Shannon TR, Duncan AM, Blatter LA & Bers DM (2011). Dynamic calcium movement inside cardiac sarcoplasmic reticulum during release. *Circ Res* **108**, 847–856.

Priori SG & Chen SR (2011). Inherited dysfunction of sarcoplasmic reticulum Ca^{2+} handling and arrhythmogenesis. *Circ Res* **108**, 871–883.

Ramay HR, Jafri MS, Lederer WJ & Sobie EA (2010). Predicting local SR Ca^{2+} dynamics during Ca^{2+} wave propagation in ventricular myocytes. *Biophys J* **98**, 2515–2523.

Ramay HR, Liu OZ & Sobie EA (2011). Recovery of cardiac calcium release is controlled by sarcoplasmic reticulum refilling and ryanodine receptor sensitivity. *Cardiovasc Res* **91**, 598–605.

Schlotthauer K & Bers DM (2000). Sarcoplasmic reticulum Ca^{2+} release causes myocyte depolarization. Underlying mechanism and threshold for triggered action potentials. *Circ Res* **87**, 774–780.

Sedej S, Heinzel FR, Walther S, Dybkova N, Wakula P, Groborz J, Gronau P, Maier LS, Vos MA, Lai FA, Napolitano C, Priori SG, Kockskamper J & Pieske B (2010). Na^{+}-dependent SR Ca^{2+} overload induces arrhythmogenic events in mouse cardiomyocytes with a human CPVT mutation. *Cardiovasc Res* **87**, 50–59.

Shan J, Betzenhauser MJ, Kushnir A, Reiken S, Meli AC, Wronska A, Dura M, Chen BX & Marks AR (2010). Role of chronic ryanodine receptor phosphorylation in heart failure and β-adrenergic receptor blockade in mice. *J Clin Invest* **120**, 4375–4387.

Shannon TR, Guo T & Bers DM (2003). Ca^{2+} scraps: local depletions of free $[Ca^{2+}]$ in cardiac sarcoplasmic reticulum during contractions leave substantial Ca^{2+} reserve. *Circ Res* **93**, 40–45.

Stern MD, Capogrossi MC & Lakatta EG (1988). Spontaneous calcium release from the sarcoplasmic reticulum in myocardial cells: mechanisms and consequences. *Cell Calcium* **9**, 247–256.

Stokke MK, Briston SJ, Jolle GF, Manzoor I, Louch WE, Oyehaug L, Christensen G, Eisner DA, Trafford AW, Sejersted OM & Sjaastad I (2010*a*). Ca^{2+} wave probability is determined by the balance between SERCA2-dependent Ca^{2+} reuptake and threshold SR Ca^{2+} content. *Cardiovasc Res* **90**, 503–512.

Stokke MK, Hougen K, Sjaastad I, Louch WE, Briston SJ, Enger UH, Andersson KB, Christensen G, Eisner DA, Sejersted OM & Trafford AW (2010*b*). Reduced SERCA2 abundance decreases the propensity for Ca^{2+} wave development in ventricular myocytes. *Cardiovasc Res* **86**, 63–71.

Swietach P, Spitzer KW & Vaughan-Jones RD (2008). Ca^{2+}-mobility in the sarcoplasmic reticulum of ventricular myocytes is low. *Biophys J* **95**, 1412–1427.

Swietach P, Spitzer KW & Vaughan-Jones RD (2010). Modeling calcium waves in cardiac myocytes: importance of calcium diffusion. *Front Biosci* **15**, 661–680.

Terentyev D, Gyorke I, Belevych AE, Terentyeva R, Sridhar A, Nishijima Y, de Blanco EC, Khanna S, Sen CK, Cardounel AJ, Carnes CA & Gyorke S (2008). Redox modification of ryanodine receptors contributes to sarcoplasmic reticulum Ca^{2+} leak in chronic heart failure. *Circ Res* **103**, 1466–1472.

Tsien RW, Bean BP, Hess P, Lansman JB, Nilius B & Nowycky MC (1986). Mechanisms of calcium channel modulation by β-adrenergic agents and dihydropyridine calcium agonists. *J Mol Cell Cardiol* **18**, 691–710.

Ullrich ND, Valdivia HH & Niggli E (2012). PKA phosphorylation of cardiac ryanodine receptor modulates SR luminal Ca^{2+} sensitivity. *J Mol Cell Cardiol* **53**, 33–42.

van Oort RJ, McCauley MD, Dixit SS, Pereira L, Yang Y, Respress JL, Wang Q, De Almeida AC, Skapura DG, Anderson ME, Bers DM & Wehrens XH (2010). Ryanodine receptor phosphorylation by calcium/calmodulin-dependent protein kinase II promotes life-threatening ventricular arrhythmias in mice with heart failure. *Circulation* **122**, 2669–2679.

Venetucci LA, Trafford AW & Eisner DA (2007). Increasing ryanodine receptor open probability alone does not produce arrhythmogenic calcium waves: threshold sarcoplasmic reticulum calcium content is required. *Circ Res* **100**, 105–111.

Wehrens XH, Lehnart SE, Reiken S, Vest JA, Wronska A & Marks AR (2006). Ryanodine receptor/calcium release channel PKA phosphorylation: a critical mediator of heart failure progression. *Proc Natl Acad Sci U S A* **103**, 511–518.

Yamaguchi N & Meissner G (2007). Does Ca^{2+}/calmodulin-dependent protein kinase δ_c activate or inhibit the cardiac ryanodine receptor ion channel? *Circ Res* **100**, 293–295.

Zhou P, Zhao YT, Guo YB, Xu SM, Bai SH, Lakatta EG, Cheng H, Hao XM & Wang SQ (2009). β-Adrenergic signalling accelerates and synchronizes cardiac ryanodine receptor response to a single L-type Ca^{2+} channel. *Proc Natl Acad Sci U S A* **106**, 18028–18033.

Zima AV, Bovo E, Bers DM & Blatter LA (2011). Ca^{2+} spark-dependent and -independent sarcoplasmic reticulum Ca^{2+} leak in normal and failing rabbit ventricular myocytes. *J Physiol* **588**, 4743–4757.

Zima AV, Picht E, Bers DM & Blatter LA (2008). Termination of cardiac Ca^{2+} sparks: role of intra-SR $[Ca^{2+}]$, release flux, and intra-SR Ca^{2+} diffusion. *Circ Res* **103**, e105–115.

Author contributions

T.L.D., J.T.M. and L.A.B. contributed to the conception and design of the study, analysis and interpretation of data, and writing of the article, and have approved the final version of the manuscript. T.L.D. and J.T.M. performed the experimental work.

Acknowledgements

This work was supported by National Institutes of Health grants HL62231, HL80101 and HL101235 (to L.A.B.) and F32HL090211 (to T.L.D.) and the Leducq Foundation (to L.A.B.). The authors would also like to thank Dr Elisa Bovo, Stephen Shonts and Demetrio Santiago for assistance with myocyte isolation.

Author's present address

Timothy L. Domeier: Department of Medical Pharmacology and Physiology, University of Missouri School of Medicine, Columbia, MO 65212, USA.